American Mineralogist, Volume 98, pages 297–303, 2013

Fluor-elbaite, $Na(Li_{1.5}Al_{1.5})Al_6(Si_6O_{18})(BO_3)_3(OH)_3F$, a new mineral species of the tourmaline supergroup

Ferdinando Bosi,[1,*] Giovanni B. Andreozzi,[1] Henrik Skogby,[2] Aaron J. Lussier,[3] Yassir Abdu,[3] and Frank C. Hawthorne[3]

[1]Dipartimento di Scienze della Terra, Sapienza Università di Roma, P.le A. Moro, 5, I-00185 Rome, Italy
[2]Department of Mineralogy, Swedish Museum of Natural History, Box 50007, SE-10405 Stockholm, Sweden
[3]Department of Geological Sciences, University of Manitoba, Winnipeg, Manitoba R3T 2N2, Canada

Abstract

Fluor-elbaite, $Na(Li_{1.5}Al_{1.5})Al_6(Si_6O_{18})(BO_3)_3(OH)_3F$, is a new mineral of the tourmaline supergroup. It is found in miarolitic cavities in association with quartz, pink muscovite, lepidolite, spodumene, spessartine, and pink beryl in the Cruzeiro and Urubu mines (Minas Gerais, Brazil), and apparently formed from late-stage hydrothermal solutions related to the granitic pegmatite. Crystals are blue-green with a vitreous luster, sub-conchoidal fracture and white streak. Fluor-elbaite has a Mohs hardness of approximately 7.5, and has a calculated density of about 3.1 g/cm^3. In plane-polarized light, fluor-elbaite is pleochroic (O = green/bluish green, E = pale green), uniaxial negative. Fluor-elbaite is rhombohedral, space group *R*3*m*, *a* = 15.8933(2), *c* = 7.1222(1) Å, *V* = 1558.02(4) Å^3, *Z* = 3 (for the Cruzeiro material). The strongest eight X-ray-diffraction lines in the powder pattern [*d* in Å(*I*)(*hkl*)] are: 2.568(100)(051), 2.939(92)(122), 3.447(67)(012), 3.974(58)(220), 2.031(57)(152), 4.200(49)(211), 1.444(32)(642), and 1.650(31)(063). Analysis by a combination of electron microprobe, secondary ion mass spectrometry, and Mössbauer spectroscopy gives SiO_2 = 37.48, Al_2O_3 = 37.81, FeO = 3.39, MnO = 2.09, ZnO = 0.27, CaO = 0.34, Na_2O = 2.51, K_2O = 0.06, F = 1.49, B_2O_3 = 10.83, Li_2O = 1.58, H_2O = 3.03, sum 100.25 wt%. The unit formula is: $^X(Na_{0.78}\square_{0.15}Ca_{0.06}K_{0.01})^Y(Al_{1.15}Li_{1.02}Fe^{2+}_{0.46}Mn^{2+}_{0.28}Zn_{0.03})$ $^Z(Al_6)^T(Si_{6.02}O_{18})^B(BO_3)_3{}^V(OH)_3{}^W(F_{0.76}OH_{0.24})$.

The crystal structure of fluor-elbaite was refined to statistical indices *R*1 for all reflections less then 2% using Mo*K*α X-ray intensity data. Fluor-elbaite shows relations with elbaite and tsilaisite through the substitutions ^{W}F ↔ ^{W}OH and ^{Y}(Al + Li) + ^{W}F ↔ 2^{Y}Mn^{2+} + ^{W}OH, respectively.

Keywords: Fluor-elbaite, tourmaline, new mineral species, crystal-structure refinemnet, electron microprobe, ion microprobe, Mössbauer spectroscopy

Introduction

The tourmaline supergroup minerals occur typically as accessory phases (but occasionally as minor or even major minerals) in a wide range of rocks of different origin and composition, including granitic pegmatites. They are well known as valuable indicator minerals that can provide information on the compositional evolution of their host rocks, chiefly due to their ability to incorporate a large number of elements (e.g., Novák et al. 2004, 2011; Agrosì et al. 2006; Lussier et al. 2011a; van Hinsberg et al. 2011). However, the chemical composition of tourmalines is also strongly controlled by various crystal-structural constraints (e.g., Hawthorne 1996, 2002; Bosi 2010, 2011; Henry and Dutrow 2011) as well as by temperature (van Hinsberg and Schumacher 2011).

The crystal structure and crystal chemistry of tourmaline have been extensively studied (e.g., Foit 1989; Hawthorne 1996; Hawthorne and Henry 1999; Bosi and Lucchesi 2007; Lussier et al. 2008, 2011a, 2011b; Bosi et al. 2010). The general formula of tourmaline may be written as: $XY_3Z_6T_6O_{18}(BO_3)_3V_3W$, where X (≡ $^{[9]}X$) = Na^+, K^+, Ca^{2+}, □ (= vacancy); Y (≡ $^{[6]}Y$) = Al^{3+}, Fe^{3+}, Cr^{3+}, V^{3+}, Mg^{2+}, Fe^{2+}, Mn^{2+}, Li^+; Z (≡ $^{[6]}Z$) = Al^{3+}, Fe^{3+}, Cr^{3+}, V^{3+}, Mg^{2+}, Fe^{2+}; T (≡ $^{[4]}T$) = Si^{4+}, Al^{3+}, B^{3+}; B (≡ $^{[3]}B$) = B^{3+}; W (≡ $^{[3]}$O1) = OH^{1-}, F^{1-}, O^{2-}; V (≡ $^{[3]}$O3) = OH^{1-}, O^{2-} and where, for example, T represents a group of cations (Si^{4+}, Al^{3+}, B^{3+}) accommodated at the [4]-coordinated *T* sites. The dominance of such ions at one or more sites of the structure gives rise to many distinct mineral species (Henry et al. 2011).

A previous study on the crystal chemistry of the tourmaline-supergroup minerals (Federico et al. 1998) demonstrated the presence of the "fluor-" equivalent of elbaite in the Cruzeiro mine (Minas Gerais, Brazil). Moreover, the fluor-elbaite end-member was predicted by Hawthorne and Henry (1999) with the ideal formula $Na(Li_{1.5}Al_{1.5})Al_6Si_6O_{18}(BO_3)_3(OH)_3F$, derived from the root composition of elbaite, $Na(Li_{1.5}Al_{1.5})Al_6(Si_6O_{18})(BO_3)_3(OH)_3OH$, via the substitution F → OH at the W position.

A formal description of the new species fluor-elbaite is presented here, including a full characterization of its physical, chemical, and structural attributes. The name has been assigned according to the chemical composition, as recommended by Henry et al. (2011). The new species as well as the new name have been approved by the Commission on New Minerals, Nomenclature and Classification of the International Mineralogical

* E-mail: ferdinando.bosi@uniroma1.it

0003-004X/13/0203–297$05.00/DOI: http://dx.doi.org/10.2138/am.2013.4285

Association (IMA 2011-071). The holotype specimen from the Cruzeiro mine is deposited in the collections of the Museum of Mineralogy, Earth Sciences Department, Sapienza University of Rome, Italy, catalog number 33045. The holotype specimen from the Urubu mine is deposited in the collection of the Department of Natural History, Royal Ontario Museum, Canada, catalog number M56418.

Occurrence, appearance, physical and optical properties

The fluor-elbaite specimens here examined occur at two deposits. The first one is the Cruzeiro mine (São José da Safira, Minas Gerais, Brazil), where tourmaline is associated with quartz, pink muscovite, lepidolite, spodumene, spessartine, and pink beryl (Federico et al. 1998). The mineral is also found in the Urubu mine (Itinga, Minas Gerais, Brazil), but in this case associated minerals are not known. Both the Cruzeiro and Urubu fluor-elbaite crystals formed from late-stage hydrothermal solutions inside (or close to) miarolitic cavities of the granitic pegmatite (e.g., Federico et al. 1998). The crystal from Cruzeiro is a euhedral, inclusion-free, blue-green, elongated prism. It was cut in slices for analytical purposes. The remaining slice is approximately 4 × 4 × 1 mm in size (Fig. 1). The crystal from Urubu is a euhedral, blue-green, elongated prism approximately 1.3 × 1.2 × 2.3 cm in size.

The fluor-elbaite morphology consists of elongated $\{10\bar{1}0\}$ and $\{11\bar{2}0\}$ prisms with striated faces terminated by a prominent {0001} pedion (Fig. 2). The crystals are brittle with a vitreous luster, sub-conchoidal fracture, and white streak; Mohs hardness is approximately 7.5. The calculated density is 3.091 g/cm^3 (Cruzeiro) and 3.123 g/cm^3 (Urubu). In transmitted light, the investigated fluor-elbaite samples are pleochroic with O = green and E = pale green (Cruzeiro) and O = bluish green and E = pale green (Urubu). Fluor-elbaite is uniaxial negative with refractive indices of ω = 1.640(5), ε = 1.625(5) measured by the immersion method using white light from a tungsten source (Cruzeiro), and ω = 1.648(2), ε = 1.629(2) measured with gel-filtered Na light (λ = 589.9 nm) (Urubu). The mean index of refraction, density, and chemical composition lead to excellent (Cruzeiro) and superior (Urubu) compatibility indices ($1 - K_p/K_c$ = 0.026 and 0.018, respectively) (Mandarino 1976, 1981).

It is worth pointing out that the blue-green bulk color as well as the pleochroism observed for the present crystals is most likely caused by minor concentrations of chromophores (e.g., Fe and Mn). Presumably, end-member fluor-elbaite will be colorless.

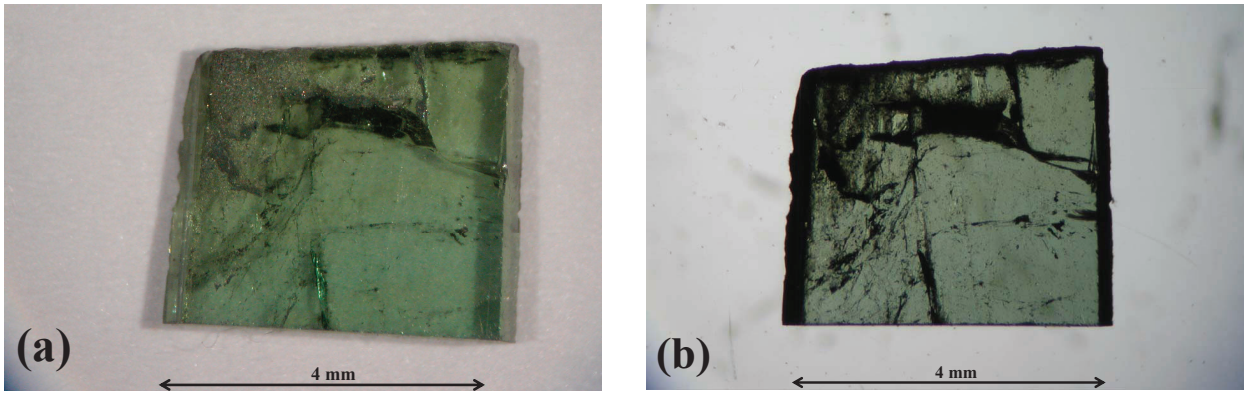

Figure 1. Photos of the holotype fragment of fluor-elbaite from Cruzeiro (Brazil) in reflected (**a**) and transmitted (**b**) light.

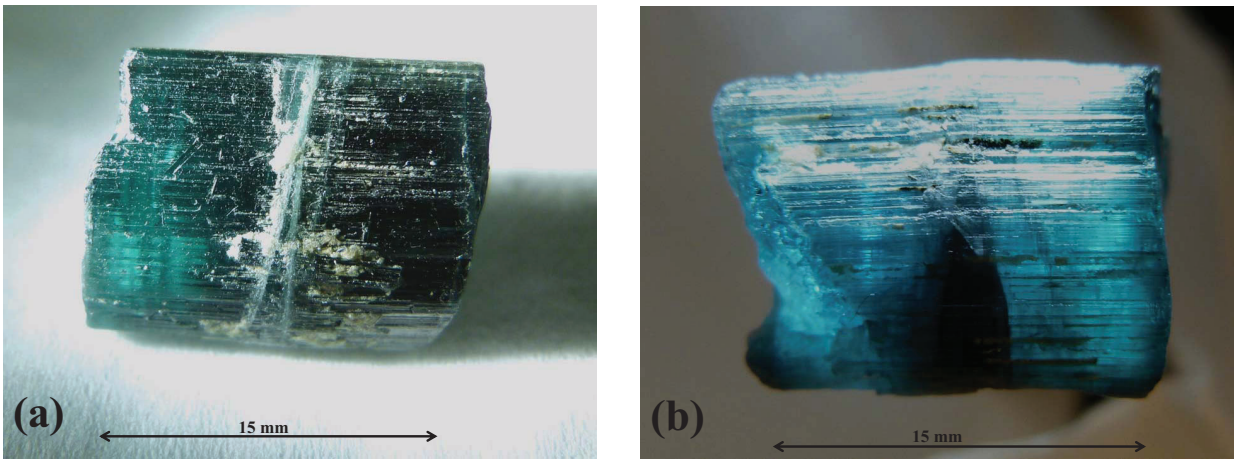

Figure 2. Photos of a representative crystal of fluor-elbaite (unknown locality) in reflected (**a**) and transmitted (**b**) light.

TABLE 1. Chemical composition of fluor-elbaite

Sample	Cruzeiro		Urubu	
	Average	Probe standard	Average	Probe standard
SiO_2 wt%	37.48(18)	Wollastonite	36.70(17)	Diopside
B_2O_3	10.83(56)*	Elbaite	10.73(6)‡	
Al_2O_3	37.81(18)	Corundum	37.73(12)	Andalusite
FeO	3.39(10)†	Magnetite	6.69(8)†	Fayalite
MnO	2.09(9)	Metallic Mn	0.64(3)	Spessartine
ZnO	0.27(9)	Metallic Zn	0.53(4)	Gahnite
CaO	0.34(5)	Wollastonite	0.10(1)	Diopside
Na_2O	2.51(5)	Jadeite	2.65(4)	Albite
K_2O	0.06(2)	Orthoclase	bdl	Orthoclase
Li_2O	1.58(10)*	Elbaite	1.14(5)‡	
F	1.49(10)	Fluorphlogopite	1.37(11)	Fluororiebeckite
H_2O	3.03‡		2.95(5)*	Elbaite
–O=F	–0.63		–0.58	
Total	100.25		100.67	
Atomic proportions normalized to 31 anions				
Si apfu	6.02(5)		5.94(2)	
B	3.0(1)		3.0(1)	
Al	7.15(6)		7.20(4)	
Fe^{2+}	0.46(1)		0.91(1)	
Mn^{2+}	0.28(1)		0.09(1)	
Zn	0.03(1)		0.06(1)	
Ca	0.06(1)		0.02(1)	
Na	0.78(2)		0.83(1)	
K	0.012(4)		–	
Li	1.02(6)		0.74(3)	
F	0.76(5)		0.70(5)	
OH	3.24		3.19(4)	

Notes: Standard errors for the atomic proportions (in parentheses) were calculated by error-propagation theory. Ti and Mg were found to be below their respective detection limits (0.03 wt%). bdl = below detection limits, apfu = atoms per formula unit.
* Measured by secondary-ion mass spectrometry.
† Measured as Fe^{2+} by Mössbauer spectroscopy.
‡ Calculated by stoichiometry. In detail, the B_2O_3 and Li_2O contents for the Urubu sample were calculated on the same basis of B = 3 apfu and Li apfu = 9 – Σ(Y + Z); the H_2O content for the Cruzeiro sample was calculated on the basis of OH + F = 4 apfu.

METHODS

Microprobe analysis

Cruzeiro. Chemical data for the fluor-elbaite from Cruzeiro were reported by Federico et al. (1998) when describing sample 95V. In detail, 10 chemical spot analyses were done using an electron microprobe in WDS mode (15 kV, 15 nA, 5 μm beam diameter). The light elements H, Li, and B were analyzed by an ion microprobe (secondary ion mass spectrometry, primary current of oxygen negative, with an intensity of 5 nA, focused on 10 μm, secondary current of positive ions, voltage offset of –60 V energy window of 10 V) after calibration against TG and AAS data for H and Li, respectively, as well as against glasses and tourmaline samples for B (Federico et al. 1998). However, the measured H_2O content was relatively high (3.34 ± 0.16 wt%), and would give an anomalous excess of OH+F (4.31 ± 0.17 apfu) in the tourmaline formula. Consequently, H_2O content was calculated by stoichiometry (3.03 apfu, Table 1). Note that the difference between the measured and calculated H_2O values is within the analytical error (2σ).

Urubu. Chemical data for fluor-elbaite from Urubu were obtained primarily using a Cameca SX100 electron microprobe (10 chemical spot analyses in WDS mode, 15 kV, 10 nA, 10 μm beam diameter). Li_2O and B_2O_3 were calculated from the stoichiometry. Hydrogen was analyzed using a Cameca 7f SIMS. The relative ion signal of H^+ was normalized to Si^+ whose concentration was measured by electron probe. Hydrogen and ^{28}Si were measured using a ~10–15 μm 6 nA primary beam of $^{16}O^-$ ions. The magnet was sequentially switched to collect hydrogen and silicon. During analytical sessions, the sample accelerating voltage was set to +9.9 kV, with electrostatic analyzer in the secondary column set to accept +10 kV and an energy window of ±50 volts. This voltage offset was sufficient to suppress isobaric interferences during analysis. The entrance slit was narrowed to obtain flat-top peaks at a mass resolving power of about 400. Ions were detected with a Balzers SEV 1217 electron multiplier coupled with an ion-counting system with an overall deadtime of 37 ns. The amount of H was quantified using elbaite and cordierite of known chemical compositions. Analytical data are summarized in Table 1.

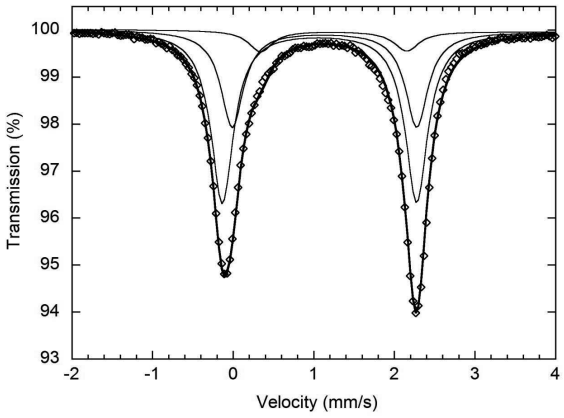

FIGURE 3. Room-temperature Mössbauer spectrum of fluor-elbaite (Cruzeiro), fitted with three doublets (thin lines) assigned to Fe^{2+} (centroid shifts: 1.07, 1.13, 1.24 mm/s; quadrupole splittings: 2.41, 2.29, 1.82 mm/s, respectively, relative to α-Fe foil). Thick line denotes summed spectrum.

Mössbauer spectroscopy

Cruzeiro. The oxidation state of Fe was determined by Mössbauer spectroscopy at room temperature using a conventional spectrometer system operating in constant-acceleration mode. To save sample material, the absorber was prepared by filling a small quantity of ground material in a 1 mm hole in a lead plate, and the spectrum was acquired using a ^{57}Co point-source in rhodium matrix with a nominal activity of 10 mCi. The spectrum was calibrated against α-Fe foil and folded before fitting using the MDA software by Jernberg and Sundqvist (1983). The resultant spectrum (Fig. 3) shows an asymmetric doublet with hyperfine parameters typical for Fe^{2+}, but no indications of Fe^{3+}. To account for the asymmetry, the spectrum was fitted with three doublets assigned to Fe^{2+}; however, these three doublets are not well-resolved and were not considered as representing three distinctly different Fe^{2+} environments in the tourmaline structure.

Urubu. Mössbauer spectroscopy measurements were done in transmission geometry at room temperature (RT) using a $^{57}Co(Rh)$ point source. The spectrometer was calibrated with the RT spectrum of α-Fe. In preparing the Mössbauer absorber, fluor-elbaite was mixed with sugar and finely ground under acetone to avoid oxidation. The mixture was then loaded into a Pb ring (2 mm inner diameter) and covered by tape on both sides. Assuming a recoilless fraction of 0.7 for the Mössbauer absorber, the amount of sample corresponds to an absorber thickness of ~4 mg Fe/cm^2). The spectra were analyzed using a Voigt-based quadrupole-splitting distribution (QSD) method (Rancourt and Ping 1991). To account for absorber thickness effects, we allowed the Lorentzian linewidth (Γ) of the symmetrical elemental doublets of the QSD to be an adjustable parameter during the spectrum fitting (Rancourt 1994). However, full thickness correction was applied to the Mössbauer data (Rancourt et al. 1993) and similar results (Fe^{3+}/Fe^{2+}) were obtained from fitting of the thickness-corrected spectrum. The RT Mössbauer spectrum of the Urubu fluor-elbaite (not shown) was also fitted by a model having three general sites for Fe^{2+} with no indication of Fe^{3+}, in full agreement with that of the Cruzeiro sample.

X-ray powder diffraction

Cruzeiro. The X-ray powder-diffraction pattern for the sample from Cruzeiro was collected using a Panalytical X'pert powder diffractometer equipped with an X'celerator silicon-strip detector. The diffraction data (in Å for CuK, λ = 1.54060 Å), corrected using Si as an internal standard, are listed in Table 2. Unit-cell parameters from the powder data were refined using the program UnitCell (Holland and Redfern 1997): a = 15.8970(6), c = 7.1227(3) Å, V = 1558.9(1) Å^3.

Urubu. X-ray powder-diffraction data for the sample from Urubu were collected with a Bruker D8 Discover SuperSpeed micro-powder diffractometer with a multi-wire 2D detector using a modified Gandolfi attachment, and indexed on a = 15.915(3), c = 7.120(2) Å, V = 1561.8(7) Å^3. Data (in angstroms for Cu$K\alpha$) are listed in Table 2.

Single-crystal structural refinement (SREF)

Cruzeiro. A representative crystal of the type specimen was selected for X-ray diffraction measurements on a Bruker KAPPA APEX-II single-crystal diffractometer (Sapienza University of Rome, Earth Sciences Department), equipped with a CCD area detector (6.2 × 6.2 cm^2 active detection area, 512 × 512 pixels) and a graphite-crystal monochromator, using Mo$K\alpha$ radiation from a fine-focus sealed X-ray tube. The sample-to-detector distance was 4 cm. A total of 4830 exposures (step = 0.2°, time/step = 20 s) covering a full reciprocal sphere with a redundancy of about 10 were collected and a completeness of 99.7% was achieved. The orientation of the crystal lattice was determined using more than 700 strong reflections, $I > 100\ \sigma(I)$ evenly distributed in reciprocal space, and used for subsequent integration of all recorded intensities. Final unit-cell parameters were refined by using the Bruker AXS SAINT program on reflections with $I > 10\sigma(I)$ in the range $6° < 2\theta < 81°$. The intensity data were processed and corrected for Lorentz, polarization, and background effects with the APEX2 software program of Bruker AXS. The data were corrected for absorption using a multi-scan method (SADABS). The absorption correction led to a significant improvement in R_{int}. No violations of $R3m$ symmetry were noted.

Structure refinement was done with the SHELXL-97 program (Sheldrick 2008). Starting coordinates were taken from Bosi et al. (2010). Variable parameters were: scale factor, extinction coefficient, atomic coordinates, site-scattering values expressed as mean atomic number (for X and Y sites) and atomic displacement factors. To obtain the best values of statistical indexes ($R1$, w$R2$), a fully ionized O scattering curve was used, whereas neutral scattering curves were used for the other atoms. In detail, the X site was modeled using the Na scattering factor. The occupancy of the Y site was obtained considering the presence of Fe vs. Li. The Z, T, B, and O1 sites were modeled, respectively, with Al, Si, B, and F scattering factors and with a fixed occupancy of 1, because refinement with unconstrained occupancies showed no significant deviations from this value. Following the findings of Burns et al. (1994) who reported high U_{eq} values for the O1 and O2 sites that indicate position disorder, the crystal was refined twice, (1) with both sites constrained to their positions of maximum site-symmetry, (00z) for O1 and (x, 1–x, z) for O2, and (2) with both sites allowed to disorder with coordinates (x, x/2, z) and (x,y,z) (referred as split-site SREF in this work). There were no correlations greater than 0.7 between the parameters at the end of the refinement. Table 3 lists crystal data, data collection information, and refinement details; Table 4 gives the fractional atomic coordinates, equivalent isotropic displacement parameters; Table 5[1] (on deposit) contains anisotropic displacement parameters; Table 6 shows selected bond lengths.

Urubu. A single crystal was mounted on a Bruker D8 three-circle diffractometer equipped with a rotating anode generator (Mo$K\alpha$ X-radiation), multi-layer optics and an APEX-II CCD detector. The intensities of 7994 reflections were collected to 60° 2θ using 20s per 0.2° frame with a crystal-to-detector distance of 5 cm. Empirical absorption corrections (SADABS; Sheldrick 1996) were applied and identical data merged. Unit-cell parameters were obtained by least-squares refinement of >1000 reflections [$I > 10\sigma(I)$] and are given in Table 3.

The SHELXL-97 software package (Sheldrick 2008) was used for refinement of the Urubu fluor-elbaite crystal structure. Starting coordinates were taken from a crystal described in Lussier et al. (2011b). Fully ionized scattering factors for O^{2-} were used, whereas neutral scattering factors for all other atoms were used, following the findings presented in Lussier et al. (2011b) that showed best agreement between chemical and structural data using these particular scattering factors. The X-site was modeled using the Na scattering factor and the occupancy

TABLE 2. X-ray powder diffraction data for fluor-elbaite

Cruzeiro				Urubu			
I_{meas} %	$h\,k\,l$	d_{meas} Å	d_{calc} Å	I_{meas} %	$h\,k\,l$	d_{meas} Å	d_{calc} Å
17	1 0 1	6.318	6.326	4	$\bar{1}$ 2 0	7.977	7.958
18	0 2 1	4.950	4.950	32	$\bar{1}$ 1 1	6.332	6.326
12	0 3 0	4.587	4.589	32	0 2 1	4.957	4.952
49	2 1 1	4.200	4.202	20	0 3 0	4.598	4.594
58	2 2 0	3.974	3.974	66	$\bar{2}$ 3 1	4.206	4.204
67	0 1 2	3.447	3.448	78	$\bar{2}$ 4 0	3.977	3.979
14	1 3 1	3.365	3.365	60	0 1 2	3.449	3.447
14	4 1 0	3.004	3.004	17	$\bar{1}$ 4 1	3.369	3.368
92	1 2 2	2.939	2.939	5	$\bar{4}$ 4 1	3.101	3.102
6	3 2 1	2.885	2.887	16	$\bar{1}$ 5 0	3.006	3.008
8	3 1 2	2.604	2.604	81	$\bar{1}$ 3 2	2.939	2.939
100	0 5 1	2.568	2.568	100	0 5 1	2.569	2.571
16	0 0 3	2.374	2.374	2	0 4 2	2.478	2.476
22	5 1 1	2.336	2.336	3	$\bar{2}$ 6 1	2.447	2.446
11	5 0 2	2.178	2.178	27	0 0 3	2.367	2.373
15	4 3 1	2.157	2.157		$\bar{2}$ 5 2	2.367	2.364
17	0 3 3	2.109	2.109	24	$\bar{5}$ 6 1	2.342	2.338
27	2 2 3	2.038	2.038	4	0 6 0	2.295	2.297
57	1 5 2	2.031	2.031	22 B	$\bar{5}$ 5 2	2.161*	
7	1 6 1	2.014	2.014		$\bar{4}$ 7 1	2.161*	
3	4 4 0	1.986	1.987	24	$\bar{3}$ 3 3	2.107	2.109
23	3 4 2	1.910	1.910		0 3 3	2.107	2.109
8	1 4 3	1.862	1.863		$\bar{4}$ 6 2	2.107	2.102
10	1 0 4	1.767	1.766	69	$\bar{2}$ 4 3	2.034	2.038
31	0 6 3	1.650	1.650		$\bar{1}$ 6 2	2.034	2.032
21	5 5 0	1.590	1.590	5	$\bar{4}$ 8 0	1.990	1.989
8	4 5 2	1.581	1.580	43	$\bar{3}$ 7 2	1.911	1.912
24	0 5 4	1.495	1.495	9	$\bar{1}$ 5 3	1.862	1.863
32	6 4 2	1.445	1.444	12	$\bar{6}$ 8 1	1.847	1.846
9	0 1 5	1.417	1.417	10	$\bar{3}$ 6 3	1.768	1.769
11	6 5 1	1.414	1.414		$\bar{1}$ 1 4	1.768	1.765
23	4 3 4	1.399	1.399	4	0 2 4	1.723	1.723
					$\bar{5}$ 8 2	1.723	1.723
				4	$\bar{2}$ 8 2	1.684	1.684
				28 B	$\bar{6}$ 6 3	1.649	1.651
					0 6 3	1.649	1.651
				24 B	$\bar{2}$ 9 1	1.639	1.639
				23 B	$\bar{5}$ 10 0	1.590	1.592
				4B	$\bar{4}$ 10 1	1.545*	
					0 9 0	1.545*	
				6B	$\bar{7}$ 9 2	1.522*	
					$\bar{7}$ 10 1	1.522*	
				12	0 5 4	1.496	1.495

Notes: I_{meas} = measured intensity, d_{meas} = measured interplanar spacing; d_{calc} = calculated interplanar spacing; hkl = reflection indices. Estimated errors in d_{meas}-spacing range from 0.01 Å for large d-values to 0.001 Å for small d-values. * Not used in refinement; B = broad.

TABLE 3. Single-crystal X-ray diffraction data details for fluor-elbaite

	Cruzeiro		Urubu	
Crystal size (mm)	0.30 × 0.32 × 0.33		0.14 x 0.15 x 0.10	
Unit-cell parameter a (Å)	15.8933(2)		15.9083(6)	
Unit-cell parameter c (Å)	7.1222(1)		7.1229(3)	
Unit-cell volume (Å^3)	1558.02(4)		1561.12(19)	
Range for data collection, 2θ (°)	5–81		5–60	
Reciprocal space range hkl	$-28 \le h \le 28$		$-22 \le h \le 22$	
	$-28 \le k \le 20$		$-22 \le k \le 22$	
	$-12 \le l \le 12$		$-9 \le l \le 10$	
Total number of frames	4830		4580	
Set of measured reflections	12117		7994	
Unique reflections, R_{int} (%)	2279, 2.11		4617, 2.22	
Absorption correction method	SADABS		SADABS	
Refinement method	Full-matrix least-squares on F^2		Full-matrix least-squares on F^2	
Structural refinement program	SHELXL-97		SHELX-97	
	Standard SREF	Split-site SREF	Standard SREF	Split-site SREF
Extinction coefficient	0.0042(2)	0.0041(2)	0.0036(2)	0.0034(2)
Flack parameter	0.22(1)	0.22(1)	0.01(3)	0.02(3)
w$R2$ (%)	4.40	3.75	4.58	4.29
$R1$ (%) all data	1.87	1.50	1.90	1.75
$R1$ (%) for $I > 2\sigma_I$	1.84	1.48	1.90	1.75
GooF	1.070	1.094	1.136	1.175
Diff. peaks (±e^-/Å^3)	2.25; −1.06	0.71; −0.48	0.87; −0.42	0.32; −0.30

Notes: Standard and split-site SREF denote, respectively, structural refinements carried out with the O1 site at (0,0,z) and the O2 site at (x,2x,z), and with O1 at (x,2x,z) and O2 at (x,y,z) to allow for positional disorder, as indicated by the high U_{eq} values (Burns et al. 1994). R_{int} = merging residual value; $R1$ = discrepancy index, calculated from F-data; w$R2$ = weighted discrepancy index, calculated from F^2-data; GooF = goodness of fit; Diff. peaks = maximum and minimum residual electron density. Radiation, Mo$K\alpha$ = 0.71073 Å. Data collection temperature = 293 K. Space group $R3m$; $Z = 3$.

[1] Deposit item AM-13-027, CIFs and Table 5. Deposit items are available two ways: For a paper copy contact the Business Office of the Mineralogical Society of America (see inside front cover of recent issue) for price information. For an electronic copy visit the MSA web site at http://www.minsocam.org, go to the *American Mineralogist* Contents, find the table of contents for the specific volume/issue wanted, and then click on the deposit link there.

TABLE 4. Fractional atomic coordinates (*x,y,z*) and equivalent (U_{eq}) displacement parameters for fluor-elbaite (Å^2)

		Standard SREF				Split-site SREF			
Site	Sample	*x*	*y*	*z*	U_{eq}	*x*	*y*	*z*	U_{eq}
X	Cruzeiro	0	0	0.2362(2)	0.0215(4)	0	0	0.23648(16)	0.0205(3)
	Urubu	0	0	0.2361(4)	0.0280(9)	0	0	0.2364(3)	0.0261(8)
Y	Cruzeiro	0.12374(3)	*x*/2	0.62863(7)	0.00950(10)	0.12377(3)	*x*/2	0.62862(6)	0.00948(8)
	Urubu	0.12422(5)	*x*/2	0.62764(12)	0.0104(2)	0.12424(5)	*x*/2	0.62767(11)	0.0105(2)
Z	Cruzeiro	0.29746(2)	0.26065(2)	0.61125(5)	0.00613(5)	0.297451(16)	0.260633(17)	0.61131(4)	0.00612(4)
	Urubu	0.29770(4)	0.26081(4)	0.61147(11)	0.00787(12)	0.29768(4)	0.26081(4)	0.61157(10)	0.00779(11)
B	Cruzeiro	0.10946(5)	2*x*	0.45531(19)	0.00651(18)	0.10945(4)	2*x*	0.45525(15)	0.00665(15)
	Urubu	0.10966(11)	2*x*	0.4553(4)	0.0087(5)	0.10948(10)	2*x*	0.4553(4)	0.0092(4)
T	Cruzeiro	0.191971(16)	0.189959(17)	0	0.00505(4)	0.191977(13)	0.189963(14)	0	0.00495(4)
	Urubu	0.19200(3)	0.18999(3)	0	0.00659(11)	0.19200(3)	0.18999(3)	0	0.00646(10)
O1	Cruzeiro	0	0	0.7841(4)	0.0579(9)	0.02288(13)	*x*/2	0.7847(3)	0.0138(4)*
	Urubu	0	0	0.7849(6)	0.0596(14)	0.0238(3)	*x*/2	0.7854(5)	0.0142(10)*
O2	Cruzeiro	0.06070(4)	2*x*	0.48468(17)	0.0168(2)	0.06993(9)	0.12159(7)	0.48469(13)	0.00845(18)*
	Urubu	0.06092(7)	2*x*	0.4845(3)	0.0183(5)	0.0518(2)	0.9299(2)	0.4846(3)	0.0103(5)*
O3	Cruzeiro	0.26834(9)	*x*/2	0.50937(14)	0.01039(16)	0.26853(7)	*x*/2	0.50940(11)	0.01020(13)
	Urubu	0.26872(15)	*x*/2	0.5096(3)	0.0111(4)	0.26888(14)	*x*/2	0.5097(2)	0.0110(3)
O4	Cruzeiro	0.09316(4)	2*x*	0.07182(14)	0.00815(14)	0.09316(3)	2*x*	0.07170(11)	0.00815(12)
	Urubu	0.09316(7)	2*x*	0.0709(3)	0.0099(4)	0.09313(6)	2*x*	0.0709(2)	0.0100(3)
O5	Cruzeiro	0.18650(8)	*x*/2	0.09399(13)	0.00817(14)	0.18644(6)	*x*/2	0.09399(11)	0.00820(12)
	Urubu	0.18676(15)	*x*/2	0.0938(3)	0.0103(3)	0.18668(13)	*x*/2	0.0938(2)	0.0105(3)
O6	Cruzeiro	0.19679(5)	0.18654(5)	0.77568(9)	0.00727(10)	0.19673(4)	0.18650(4)	0.77569(8)	0.00739(8)
	Urubu	0.19723(9)	0.18700(9)	0.77565(19)	0.0089(2)	0.19722(8)	0.18699(8)	0.77565(18)	0.0089(2)
O7	Cruzeiro	0.28573(5)	0.28582(5)	0.08016(9)	0.00635(9)	0.28571(4)	0.28581(4)	0.08019(7)	0.00630(8)
	Urubu	0.28570(9)	0.28587(9)	0.08034(18)	0.0079(2)	0.28568(8)	0.28588(8)	0.08039(17)	0.0079(2)
O8	Cruzeiro	0.20986(5)	0.27041(5)	0.44124(10)	0.00762(10)	0.20983(4)	0.27046(4)	0.44134(8)	0.00755(8)
	Urubu	0.21002(10)	0.27051(10)	0.4413(2)	0.0095(3)	0.20996(9)	0.27053(9)	0.44143(18)	0.0095(2)
H3	Cruzeiro	0.2553(19)	0.1277(9)	0.390(4)	0.016*	0.2496(15)	0.1248(7)	0.394(3)	0.015*
	Urubu	0.263(3)	0.1316(13)	0.3724(5)	0.015*	0.262(2)	0.1308(12)	0.3729(5)	0.015*

Notes: Standard and split-site SREF denote, respectively, structural refinements carried out with the O1 site at (0,0,*z*) and the O2 site at (*x*,2*x*,*z*), and with O1 at (*x*,*x*/2,*z*) and O2 at (*x*,*y*,*z*) to allow for positional disorder, as indicated by the high U_{eq} values (Burns et al. 1994).
* Isotropic displacement parameter.

TABLE 6. Selected bond lengths (Å) in fluor-elbaite

	Standard SREF	
	Cruzeiro	Urubu
X-O2 (×3)	2.4340(15)	2.439(3)
X-O5 (×3)	2.7595(11)	2.765(2)
X-O4 (×3)	2.8190(12)	2.824(2)
<*X*-O>	2.671	2.677
Y-O2 (×2)	1.9743(8)	1.978(1)
Y-O6 (×2)	2.0175(7)	2.025(1)
Y-O1	2.0312(15)	2.046(2)
Y-O3	2.1640(12)	2.161(2)
<*Y*-O>	2.030	2.036
Y-O1*	1.7788(19)	1.783(4)
Y-O2 (×2)*	1.8696(11)	1.872(3)
Y-O6 (×2)*	2.0168(6)	2.025(1)
Y-O2 (×2)*	2.0862(12)	2.090(3)
Y-O3*	2.1658(10)	2.163(2)
Y-O1 (×2)*	2.1848(14)	2.204(3)
Z-O6	1.8532(7)	1.850(1)
Z-O7	1.8821(7)	1.881(1)
Z-O8	1.8848(7)	1.882(1)
Z-O8′	1.9091(7)	1.912(1)
Z-O7	1.9548(7)	1.955(1)
Z-O3	1.9624(5)	1.964(1)
<*Z*-O>	1.9077	1.907
B-O2	1.3585(18)	1.361(3)
B-O8 (×2)	1.3858(10)	1.388(2)
<*B*-O>	1.377	1.379
T-O6	1.6017(7)	1.602(1)
T-O7	1.6116(7)	1.613(1)
T-O4	1.6249(4)	1.625(1)
T-O5	1.6384(5)	1.639(1)
<*T*-O>	1.6192	1.620
O3-H3	0.87(3)	0.98†

* Bond lengths relative to the split-site SREF (see Table 4). As for the other bond lengths, they are statistically equals to the corresponding ones of the standard SREF.
† Fixed during refinement.

was allowed to refine. The *Z*, *T*, *B*, O1 sites were refined using Al, Si, B, and F scattering factors, respectively, and were held fixed at full occupancy, following the observation that removing these constraints during refinement cycles resulted in no significant deviation from full occupancy at any of these sites. Chemical analysis by electron microprobe showed the *Y* site occupancy to approximate Y = $[(Fe + Mn)_{1.0}Al_{1.2}Li_{0.8}]$, if the *Z*-site was set to Z = Al_6. Accordingly, the *Y* site was refined by setting the Fe occupancy to 1.0 atoms per formula unit (apfu) and allowing the remaining 2/3 of the site to refine as Al = (2 – Li) apfu. The position of the H atom bonded to the oxygen at the O3 position in the structure was taken from the difference-Fourier map and incorporated into the refinement model; the O3-H3 bond length was constrained to be 0.98 Å. Also this sample was refined twice according to the above-mentioned findings of Burns et al. (1994). Table 3 lists crystal data, data collection information and refinement details; Table 4 gives the fractional atomic coordinates, equivalent isotropic displacement parameters; Table 5[1] (on deposit) contains anisotropic displacement parameters; Table 6 shows selected bond lengths.

RESULTS AND DISCUSSION

In accord with the classification procedure of Henry et al. (2011), the empirical ordered formula of the studied fluor-elbaite specimens can be written as (Table 1)

$$^{X}(Na_{0.78}\square_{0.15}Ca_{0.06}K_{0.01})^{Y}(Al_{1.15}Li_{1.02}Fe^{2+}_{0.46}Mn^{2+}_{0.28}Zn_{0.03})$$
$$^{Z}Al_6{}^{T}(Si_{6.02}O_{18})^{B}(BO_3)_3{}^{V}(OH)_3{}^{W}(F_{0.76}OH_{0.24})$$

for the Cruzeiro sample and

$$^{X}(Na_{0.83}Ca_{0.02}\square_{0.15})^{Y}(Al_{1.20}Li_{0.74}Fe^{2+}_{0.91}Mn^{2+}_{0.09}Zn_{0.06})$$
$$^{Z}Al_6{}^{T}(Si_{5.94}O_{18})^{B}(BO_3)_3{}^{V}(OH)_3{}^{W}(F_{0.70}OH_{0.19}O_{0.11})$$

for the Urubu sample.

TABLE 7. Site populations and scattering factors in fluor-elbaite

Site	Sample	Site population (apfu)	Site scattering (epfu)	
			Refined	Calculated
X	Cruzeiro	0.78 Na + 0.06 Ca + 0.15 □ + 0.01 K	10.18(7)	10.00
	Urubu	0.83 Na + 0.02 Ca + 0.15 □	10.0(1)	9.6
Y	Cruzeiro	1.02 Li + 0.28 Mn^{2+} + 0.46 Fe^{2+} + 1.15 Al + 0.03 Zn	39.2(1)	38.7
	Urubu	0.74 Li + 0.09 Mn^{2+} + 0.91 Fe^{2+} + 1.20 Al + 0.06 Zn	44.1(2)	45.5
Z	Cruzeiro	6 Al	78*	78
	Urubu	6 Al	78*	78
T	Cruzeiro	6 Si	84*	84
	Urubu	6 Si	84*	84
B	Cruzeiro	3 B	15*	15
	Urubu	3 B	15*	15
O3 (≡ V)	Cruzeiro	3 (OH)	24*	24
	Urubu	3 (OH)	24*	24
O1 (≡ W)	Cruzeiro	0.24 (OH) + 0.76 F	9*	8.76
	Urubu	0.19 (OH) + 0.70 F + 0.11 O^{2-}	9*	8.7

Notes: apfu = atoms per formula unit; epfu = electrons per formula unit.
* Fixed in the final stages of refinement.

TABLE 8. Comparative data for fluor-elbaite, elbaite, and tsilaisite

	Fluor-elbaite		Elbaite	Tsilaisite
	Cruzeiro	Urubu		
a (Å)	15.8933(2)	15.9083(6)	15.86	15.9461(5)
c	7.1222(1)	7.1229(3)	7.11	7.1380(3)
V (Å³)	1558.02(4)	1561.12(19)	1548.8	1571.87(12)
Space group	*R*3*m*	*R*3*m*	*R*3*m*	*R*3*m*
Optic sign	Uniaxial (–)	Uniaxial (–)	Uniaxial (–)	Uniaxial (–)
ω	1.640(5)	1.648(2)	1.633	1.645(5)
ε	1.625(5)	1.629(2)	1.615	1.625(5)
Color	Blue-green	Blue-green	Colorless, pink, green, grey-black	Greenish yellow
Pleochroism	O = green	O = bluish green	None to very pale shades	E = pale greenish yellow
	E = pale green	E = pale green	of pink to green to grey	O = pale greenish yellow
Reference	This work	This work	www.mindat.org	Bosi et al. (2012)

These empirical formulas are consistent with the refined site-scattering values (Table 7), and show ^{Y}(2Li) contents larger than $^{Y}R^{2+}$ (divalent cations), which is typical of a ^{X}Na-, ^{Z}Al-dominant tourmaline belonging to the alkali group-subgroup 2 (Henry et al. 2011). As $^{W}F > {}^{W}OH$, the studied samples are named fluor-elbaite, referring to the ideal formula $Na(Li_{1.5}Al_{1.5})Al_6(Si_6O_{18})(BO_3)_3(OH)_3F$.

Observed <*T*-O> bond distances of Cruzeiro and Urubu fluor-elbaite (1.619 and 1.620 Å, respectively) are consistent with a *T* site fully populated by Si (MacDonald and Hawthorne 1995; Bosi and Lucchesi 2007). Observed <*Y*-O> distances of the Cruzeiro and Urubu samples (2.030 and 2.036 Å, respectively) are in very good agreement with <*Y*-O> ~2.035 Å calculated for the Y populations reported above using the ionic radii of Bosi and Lucchesi (2007). Compared to the value calculated for an ideal *Y* site populated by $(Al_{1.5}Li_{1.5})$ of <*Y*-O> ~2.005 Å, these values are significantly greater due to the occurrence of the relatively large cations Fe^{2+} and Mn^{2+} at *Y*. Furthermore, observed <*Z*-O> distances of the Cruzeiro and Urubu samples (1.908 and 1.907 Å, respectively) are perfectly in line with the value 1.907 Å expected for a *Z* site fully populated by Al (Bosi and Lucchesi 2007; Bosi 2008).

With respect to the ideal fluor-elbaite, the minor constituents in the empirical formulas are due to various substitutions: $2R^{2+} \leftrightarrow Li + Al$ (which relates to the divalent cations); $\square + 0.5Al \leftrightarrow Na + 0.5Li$ (which relates to the vacant group); $OH \leftrightarrow F$ (which relates to the hydroxy subgroup). Fluor-elbaite, besides the obvious occurrence of a solid solution with elbaite, also shows relations with tsilaisite through the ideal substitution $^{Y}(Al + Li) + {}^{W}F \leftrightarrow 2{}^{Y}Mn^{2+} + {}^{W}OH$, as already observed in a zoned tourmaline crystal from Elba Island by Bosi et al. (2012). Comparative data for fluor-elbaite, elbaite, and tsilaisite are given in Table 8.

ACKNOWLEDGMENTS

F.C.H. is grateful to Bill Pinch for loan of the fluor-elbaite specimen from the Urubu mine. A.J.L. was supported by a PGS-D (Post-Graduate Scholarship) from the Natural Sciences and Engineering Research Council of Canada; F.C.H. was supported by a Canada Research Chair in Crystallography and Mineralogy and by a Discovery grant from the Natural Sciences and Engineering Research Council of Canada, and by grants from the Canada Foundation for Innovation. Comments and suggestions by Darrell Henry, Alexander U. Falster, and the AE Aaron Celestian are appreciated.

REFERENCES CITED

Agrosì, G., Bosi, F., Lucchesi, S., Melchiorre, G., and Scandale, E. (2006) Mn-tourmaline crystals from island of Elba (Italy): Growth history and growth marks. American Mineralogist, 91, 944–952.

Bosi, F. (2008) Disordering of Fe^{2+} over octahedrally coordinated sites of tourmaline. American Mineralogist, 93, 1647–1653.

——— (2010) Octahedrally coordinated vacancies in tourmaline: a theoretical approach. Mineralogical Magazine, 74, 1037–1044.

——— (2011) Stereochemical constraints in tourmaline: from a short-range to a long-range structure. Canadian Mineralogist, 49, 17–27.

Bosi, F. and Lucchesi, S. (2007) Crystal chemical relationships in the tourmaline group: structural constraints on chemical variability. American Mineralogist, 92, 1054–1063.

Bosi, F., Balić-Žunić, T., and Surour, A.A. (2010) Crystal structure analysis of four tourmalines from the Cleopatra's Mines (Egypt) and Jabal Zalm (Saudi Arabia), and the role of Al in the tourmaline group. American Mineralogist, 95, 510–518.

Bosi, F., Skogby, H., Agrosì, G., and Scandale, E. (2012) Tsilaisite, $NaMn_3Al_6(Si_6O_{18})(BO_3)_3(OH)_3OH$, a new mineral species of the tourmaline supergroup from Grotta d'Oggi, San Pietro in Campo, island of Elba, Italy. American Mineralogist, 97, 989–994.

Burns, P.C., MacDonald, D.J., and Hawthorne, F.C. (1994) The crystal-chemistry of manganese-bearing elbaite. Canadian Mineralogist, 32, 31–41.

Federico, M., Andreozzi, G.B., Lucchesi, S., Graziani, G., and César-Mendes, J. (1998) Crystal chemistry of tourmalines. I. Chemistry, compositional variations and coupled substitutions in the pegmatite dikes of the Cruzeiro mine, Minas Gerais, Brazil. Canadian Mineralogist, 36, 415–431.

Foit, F.F. Jr. (1989) Crystal chemistry of alkali-deficient schorl and tourmaline structural relationships. American Mineralogist, 74, 422–431.

Jernberg, P. and Sundqvist, T. (1983) A versatile Mössbauer analysis program. Uppsala University, Institute of Physics (UUIP-1090).

Hawthorne, F.C. (1996) Structural mechanisms for light-element variations in tourmaline. Canadian Mineralogist, 34, 123–132.

——— (2002) Bond-valence constraints on the chemical composition of tourmaline. Canadian Mineralogist, 40, 789–797.

Hawthorne, F.C. and Henry, D. (1999) Classification of the minerals of the tourmaline group. European Journal of Mineralogy, 11, 201–215.

Henry, D.J. and Dutrow, B.L. (2011) The incorporation of fluorine in tourmaline: Internal crystallographic controls or external environmental influences? Canadian Mineralogist, 49, 41–56.

Henry, D.J., Novák, M., Hawthorne, F.C., Ertl, A., Dutrow, B.,Uher, P., and Pezzotta, F. (2011) Nomenclature of the tourmaline supergroup minerals. American Mineralogist, 96, 895–913.

Holland, T.J.B. and Redfern, S.A.T. (1997) Unit cell refinement from powder diffraction data: the use of regression diagnostics. Mineralogical Magazine, 61, 65–77.

Lussier, A.J., Aguiar, P.M., Michaelis, V.K., Kroeker, S., Herwig, S., Abdu, Y., and Hawthorne, F.C. (2008) Mushroom elbaite from the Kat Chay mine, Momeik, near Mogok, Myanmar: I. Crystal chemistry by SREF, EMPA, MAS NMR and Mössbauer spectroscopy. Mineralogical Magazine, 72, 747–761.

Lussier, A.J., Hawthorne, F.C., Aguiar, P.M., Michaelis, V.K., and Kroeker, S. (2011a) Elbaite-liddicoatite from Black Rapids glacier, Alaska. Periodico di Mineralogia, 80, 57–73.

Lussier, A.J., Abdu, Y. Hawthorne, F.C., Michaelis, V.K., Aguiar, P.M., and Kroeker, S. (2011b) Oscillatory zoned liddicoatite from Anjanabonoina, central Madagascar. I. Crystal chemistry and structure by SREF and ^{11}B and ^{27}Al MAS NMR spectroscopy. Canadian Mineralogist, 49, 63–88.

Mandarino, J.A. (1976) The Gladstone-Dale relationship. Part I: derivation of new constants. Canadian Mineralogist, 14, 498–502.

——— (1981) The Gladstone-Dale relationship. Part IV: the compatibility concept and its application. Canadian Mineralogist, 19, 441–450.

MacDonald, D.J. and Hawthorne, F.C. (1995) The crystal chemistry of Si = Al substitution in tourmaline. Canadian Mineralogist, 33, 849–858.

Novák, M., Povondra, P., and Selway, J.B. (2004) Schorl-oxy-schorl to dravite-oxy-dravite tourmaline from granitic pegmatites; examples from the Moldanubicum, Czech Republic. European Journal of Mineralogy, 16, 323–333.

Novák, M., Škoda, P., Filip, J., Macek, I., and Vaculovič T. (2011) Compositional trends in tourmaline from intragranitic NYF pegmatites of the Tøebíč Pluton, Czech Republic; electron microprobe, Mössbauer and LA-ICP-MS study. Canadian Mineralogist, 49, 359–380.

Rancourt, D.G. (1994) Mössbauer spectroscopy of minerals. I. Inadequacy of Lorentzian-line doublets in fitting spectra arising from quadrupole splitting distributions. Physics and Chemistry of Minerals, 21, 244–249.

Rancourt, D.G. and Ping, J.Y. (1991) Voigt-based methods for arbitrary shape static hyperfine parameter distributions in Mössbauer spectroscopy. Nuclear Instruments and Methods in Physics Research, B, 58, 85–97.

Rancourt, D.G., McDonald, A.M., Lalonde, A.E., and Ping, Y.J. (1993) Mössbauer absorber thicknesses for accurate site populations in Fe-bearing minerals American Mineralogist, 78, l–7.

Sheldrick, G.M. (1996) SADABS, Absorption Correction Program. University of Göttingen, Germany.

——— (2008) A short history of SHELX. Acta Crystallographica A, 64, 112–122.

van Hinsberg, V.J. and Schumacher, J.C. (2011) Tourmaline as a petrogenetic indicator mineral in the Haut-Allier metamorphic suite, Massif Central, France. Canadian Mineralogist, 49, 177–194.

van Hinsberg, V.J., Henry, D.J., and Marschall, H.R. (2011) Tourmaline: an ideal indicator of its host environment. Canadian Mineralogist, 49, 1–16.

Manuscript received July 6, 2012
Manuscript accepted October 24, 2012
Manuscript handled by Aaron Celestian